ARTICLE NO. 79-0627R

Acoustic Resonances and Sound Scattering by a Shear Layer

S. P. Koutsoyannis* and K. Karamcheti†
Stanford University, Stanford, Calif.
and
D. C. Galant‡
NASA Ames Research Center, Moffett Field, Calif.

The reflection and transmission characteristics of plane waves scattered by a finite-thickness shear layer having a linear velocity profile and bounded by two otherwise uniform parallel flows is examined using the pressure perturbation equation solutions in the shear layer that has been shown previously to be in terms of Whittaker M functions. In addition to the angle of plane wave incidence and the relative Mach number of the flows bounding the shear layer, it is found that the scattering properties of the shear layer depend crucially upon a parameter τ in such a manner that the case $\tau \to 0$ characterizes the long wavelength properties of the layer (with $\tau = 0$ being the vortex sheet) and the case $\tau \to \infty$ characterizes the short wavelength properties of the layer (geometrical acoustics). Unlike the vortex sheet, the finite-thickness shear layer was found to have no resonances or Brewster angles. Moreover, in general, for $\tau \gtrsim 0.5$ the amplified reflection regime degenerates into the total reflection regime of geometrical acoustics even in those cases in which the corresponding vortex sheet has resonances. In contrast for the region of ordinary reflection in the cases in which the corresponding vortex sheet does not have a Brewster angle, the values of the reflection coefficient up to $\tau = 2$ follow quite closely those of the votex sheet; whereas for the case for which the corresponding vortex sheet has a Brewster angle, the magnitude of the reflection coefficient may be quite sensitive to even small changes in τ in certain cases, contrary to some previous results.

Nomenclature

a	= (constant) sound speed
a_{ij}	= constant coefficients defined by Eq. (12)
b	= linear velocity profile slope [units: (time)$^{-1}$]
f,g	= the two independent solutions [Eqs. (9)] of Eq. (7)
i	$=\sqrt{-1}$
k	= wave vector of incident plane
k_x	= x component of wave vector k
m	= ¾, second index of the Whittaker M functions
p'	= pressure perturbation
$p^{(1)}, p^{(2)}$	= linear combinations of f and g
r	= position vector
sgn	= sign of
t	= time
w	= z component of the velocity perturbation
x,z	= coordinates
A,B,C,D	= expressions defined by Eqs. (14)
H	= Heaviside function
$M(z)$	= local Mach number
M_1	= upper fluid Mach number
M functions	= Whittaker M functions
R^2	= energy reflection coefficient
$\bar{R} = R_1 \pm iR_2$	= complex reflection coefficient for the perturbation velocity potential
$\bar{T} = T_1 \pm iT_2$	= complex transmission coefficient for the perturbation velocity potential
$U(z)$	= local mean speed
η	= nondimensional variable defined by Eq. (5)
θ	= incident wave angle (see Fig. 1)
κ	= $\sin\theta$
τ	= nondimensional parameter defined by Eq. (8)
ω	= angular frequency of incident plane wave
ϕ_l, ϕ_u	= perturbation velocity potentials for the lower and upper regions, respectively
φ	= transmitted wave angle

Presented as Paper 79-0627 at the AIAA 5th Aeroacoustics Conference, Seattle, Wash., March 12-14, 1979; submitted Oct. 2, 1979; revision received Feb. 6, 1980.

Index categories: Aeroacoustics; Jets, Wakes, and Viscid-Inviscid Flow Interactions; Wave Motion and Sloshing.

*Adjunct Professor, Dept. of Aeronautics and Astronautics, and Joint Institute for Aeronautics and Acoustics. Member AIAA.

†Professor, Dept. of Aeronautics and Astronautics, and Director, Joint Institute for Aeronautics and Acoustics. Associate Fellow AIAA.

‡Mathematician.

I. Introduction

THE shear layer with a linear velocity profile has been the object of a number of studies. Küchemann[1] considered the stability of the boundary layer with a linear velocity profile. Pridmore-Brown[2] studied rectangular duct modes in a duct with the basic flow having a linear velocity profile. Graham and Graham[3] studied plane wave propagation through a linear velocity profile shear layer. Goldstein and Rice[4] found an exact solution to the pressure perturbation equation in terms of linear combinations of parabolic cylinder functions of different orders. We have reported earlier[5] some general results on sound propagation through and the stability of a shear layer with a linear velocity profile using Whittaker M functions as the basic solutions of the pressure perturbation equation. Jones[6] examined the stability of such a layer for subsonic basic flow, whereas Scott[7] examined wave propagation through a linear shear layer using the Goldstein and Rice[4] complex solution. Although Jones[6] and Scott[7] have treated the more general problem of sound generation from a line source near a shear layer and thus the results should reduce to the plane wave case when the source is far from the shear layer, both dealt with subsonic basic flow whereas in this paper we are interested on acoustic resonances which occur only for supersonic flow and then only for certain combinations of the incidence angle and upper fluid

Mach number (see, for instance, Miles[8] and Ribner[9]). With the exception of Goldstein and Rice,[4] Koutsoyannis,[5] Jones,[6] and Scott,[7] the other investigators were concerned with either series or asymptotic solutions of the pressure perturbation equation in the shear layer region.

In the present study we are concerned with the behavior of the energy reflection coefficient for plane waves incident on a finite-thickness shear layer with a linear velocity profile and bounded by two uniform parallel flows. For that purpose we have numerically evaluated the solutions of the pressure perturbation equation in terms of Whittaker M functions and with the aid of these we have numerically evaluated the reflection coefficient for a number of typical cases involving the relevant parameters, i.e., the angle of incidence of the plane waves, the upper fluid Mach number, and a characteristic parameter τ which represents a nondimensional measure of the disturbance Strouhal number with respect to the disturbance Mach number in the mean flow direction.

In Sec. II we derive the expression for the reflection coefficient in terms of the two basic solutions of the pressure perturbation equation (i.e., the Whittaker M function solutions). In Sec. III we summarize and discuss our numerical results on the variation of the reflection coefficient. In Sec. IV we discuss various limiting cases including the vortex sheet and geometrical acoustics limits and in Sec. V given an analytical proof for the absence of resonances in a thin shear layer. The results of the present studies are then summarized in Sec. VI. In Appendix A we discuss the representations of the perturbations in the three flow regions (Fig. 1) and the definition of the energy reflection coefficient as well as energy conservation and in Appendix B we give the general outline of the numerical scheme used to evaluate the Whittaker M functions, particularly for large values of the argument and/or index τ.

II. Expression for Energy Reflection Coefficient

Without loss of generality we may assume that the layer with the linear velocity profile is bounded by two uniform flows, one of which is at relative rest, as shown in Fig. 1; i.e., we assume that the following two-dimensional (in the (x,z) plane) inviscid compressible shear layer is characterized by the mean piecewise continuous velocity flowfield:

$$\begin{aligned} U(z) &= 0 \quad \text{for } z \le 0 \\ &= bz \quad \text{for } 0 \le z \le z_1 \\ &= bz \quad \text{for } z_1 \le z \end{aligned} \tag{1}$$

Furthermore we assume a time-harmonic plane wave incident from the $z \le 0$ half space with wave vector $\boldsymbol{k}$ and wave number $k = \omega/a$. The entire unperturbed flowfield is otherwise assumed to be homogeneous; i.e., no variation for mean densities, temperatures, and speeds of sound are allowed.

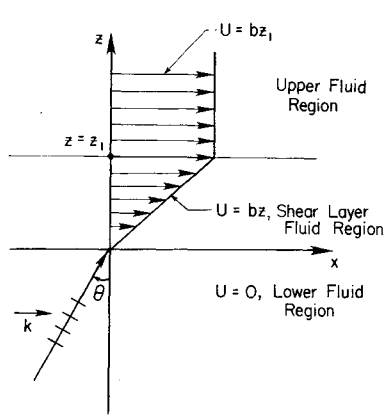

Fig. 1 Flow and incident wave geometry.

The velocity potentials ϕ_ℓ and ϕ_u in the lower and upper regions of uniform flow, respectively, bounding the shear layer of thickness z_1 may be taken to be (see, e.g., Graham and Graham[3] or Miles[8]):

$$\phi_\ell = \text{R.P.}\{\pm i\{\exp[\pm ik(x\sin\theta + z\cos\theta - at)] + \bar{R}\exp[\pm ik(x\sin\theta + z\cos\theta - at)]\}\} \text{ for } z \le 0 \tag{2}$$

$$\phi_u = \text{R.P.}\{\mp i\bar{T}\{\exp[\pm ik(x\sin\theta \pm (z - z_1)\,|\sin\theta|\sqrt{\eta_1^2 - 1} - at]\}\} \text{ for } z \ge z_1 \tag{3}$$

In the above equations R.P. denotes "real part off"; the first term in Eq. (2) represents the incident plane wave of unit amplitude emanating from the half space $z \le 0$ having wave vector $\boldsymbol{k}$ that makes an angle θ with the z axis, as shown in Fig. 1, with $-\pi/2 \le \theta \le +\pi/2$; and $\bar{R}$ and $\bar{T}$ are the complex reflection and transmission coefficients for the velocity potentials ϕ_ℓ and ϕ_u, respectively, i.e.:

$$\begin{aligned} \bar{R} &= R_1 \pm iR_2 \\ \bar{T} &= T_1 \pm iT_2 \end{aligned} \tag{4}$$

where R_i and T_i are real for the so-called ordinary and amplified reflection regimes and complex in the region of total reflection (Fig. 2). In Eqs. (2-4) the upper signs are to be used for $\eta_1 > 1$ (ordinary reflection regime), and the lower signs for $\eta_1 < -1$ (amplified reflection regime); η_1 is the nondimensional quantity $\eta_1 = (1/\sin\theta) - M_1$ [see Eq. (5)] with $M_1 = bz_1/a$ being the upper fluid Mach number. This choice of signs insures that the radiation condition, as discussed by Miles,[8] Ribner,[9] and Graham and Graham,[3] is satisfied.

In the shear layer region $0 \le z \le z_1$ in which the mean flow varies linearly with z [see Eq. (1)], it is convenient to use the nondimensional variable η (see Ref. 5)

$$\eta = \frac{1}{\sin\theta} - \frac{bz}{a} = \frac{1}{\sin\theta} - M(z) \tag{5}$$

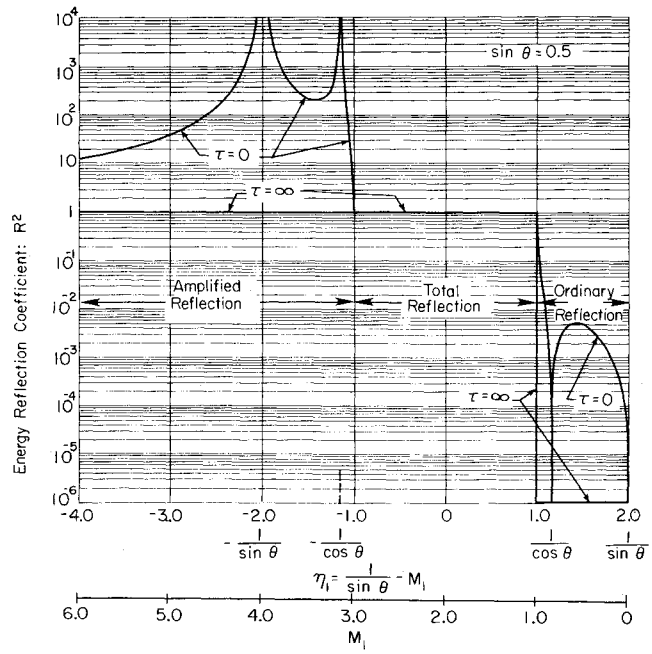

Fig. 2 Variation of energy reflection coefficient R^2 with respect to η_1, or upper fluid Mach number M_1 for an incident angle $\theta = 30$ deg for the cases of vortex sheet ($\tau = 0$) and geometrical acoustics limit ($\tau = 0$).

where $M(z)$ is the local Mach number of the mean flow in the shear layer. If one then assumes that within the shear layer region the pressure perturbation $p'(r,t)$ is of the form:

$$p'(r,t) = p(z)\begin{matrix}(\cos)\\(\sin)\end{matrix}(k_x x - \omega t) \tag{6}$$

with $k_x = \mathbf{k}\cdot\mathbf{e}_x = (\omega/a)k\sin\theta$, one obtains the following ordinary differential equation for the z-dependent part $p(z)$ of the pressure perturbation p' in terms of the nondimensional variable η defined by Eq. (5)[5]:

$$p_{\eta\eta} - (2/\eta)p_\eta + (4\tau)^2(\eta^2 - 1)p = 0 \tag{7}$$

with τ being the parameter

$$4\tau = (\omega/b)\sin\theta \tag{8}$$

We have shown earlier[5] that the two independent solutions of Eq. (7) are:

$$\left.\begin{matrix} f(\eta;\tau) \\ g(\eta;\tau) \end{matrix}\right\} = (4i\tau)^{-\frac{1}{2}\pm m}\eta^{\frac{1}{2}} M_{i\tau,\mp m}(4i\tau\eta^2), m = \tfrac{3}{4} \tag{9}$$

which are real functions of the variable η and the parameter τ for real values of η and τ. Using the above solutions $f(\eta;\tau)$ and $g(\eta;\tau)$ one may further write the following general expression for the pressure perturbation $p'(r,t)$ and the z-component w of the velocity perturbation:

$$p'(r,t) = p^{(1)}(\eta;\tau)\sin[k(x\sin\theta - at)] + p^{(2)}(\eta;\tau)\cos[k(x\sin\theta - at)] \tag{10}$$

$$w(\eta;\tau) = \frac{a}{4\tau\eta}\{p_\eta^{(1)}(\eta;\tau)\cos[k(x\sin\theta - at)] - p_\eta^{(2)}(\eta;\tau)\sin[k(x\sin\theta - at)]\} \tag{11}$$

where $p^{(1)}(\eta)$ and $p^{(2)}(\eta)$ are linear combinations of the two independent solutions $f(\eta)$ and $g(\eta)$ [given by Eqs. (9)] of the pressure perturbation equation (7), i.e.,

$$p^{(1)}(\eta;\tau) = a_{11}f(\eta;\tau) + a_{12}g(\eta;\tau),\ p^{(2)}(\eta;\tau) = a_{21}f(\eta;\tau) + a_{22}g(\eta;\tau) \tag{12}$$

where a_{ij} are constants.

Finally we apply the appropriate boundary conditions at the two edges of the shear layer, at $z=0$ and $z=z_1$ [or in terms of the nondimensional variable η [Eq. (5)] at $\eta_0 = 1/\sin\theta$ and $\eta_1 = (1/\sin\theta) - M_1$], which are the continuity of the pressure perturbation p' and of the z-component w of the velocity perturbation:

$$p'(z=0^-) = -\rho_0\frac{\partial\phi_\ell}{\partial t} = p'(z=0^+)$$

$$w(z=0^-) = (\nabla\phi_\ell)\cdot\mathbf{e}_z = w(z=0^+)$$

and similarly at $z=z_1$

$$p'(z=z_1^+) = -\rho_0\frac{\mathrm{D}\phi_u}{\mathrm{D}t} = p'(z=z_1^-)$$

$$w(z=z_1^+) = (\nabla\phi_u)\cdot\mathbf{e}_z = w(z=z_1^-)$$

with $\mathrm{D}/\mathrm{D}t$ designating the convective wave operator in the upper fluid region of constant Mach number M_1.

Then, using Eqs. (2), (3), and (10-12), one may obtain eight linear algebraic equations for the determination of the eight unknowns a_{ij}, R_i, and T_i appearing in these equations. After some tedious but straightforward algebra we obtain the following expression for the square of the reflection coefficient:

$$R^2 = \frac{(A\pm B)^2 + (C\pm D)^2}{(A\mp B)^2 + (C\mp D)^2} \quad \text{for } |\eta_1| \geq 1$$

$$|R|^2 = 1 \quad \text{for } |\eta_1| \leq 1 \tag{13}$$

where the expressions given in Eqs. (14) for A, B, C, and D involve essentially the evaluation of the two independent solutions $f(\eta)$ and $g(\eta)$ of the pressure perturbation given by Eqs. (9) and of their first derivatives at the two edges of the shear layer and are functions of $\eta_0 = 1/\sin\theta$, $\eta_1 = (1/\sin\theta) - M_1$, and the parameter τ [see Eqs. (5) and (8)]. Moreover, using Eqs. (4) for the definitions of the complex reflection and transmission coefficients $\bar{R}$ and $\bar{T}$, respectively, we easily obtain:

$$R^2 = R_1^2 + R_2^2,\quad T^2 = T_1^2 + T_2^2 \quad \text{for } |\eta_1| \geq 1$$

i.e., in the ordinary and amplified reflection regimes where R_i and T_i are real (see Fig. 2). In the total reflection regime $|\eta_1| \leq 1$, R_i and T_i are complex and it is also easily obtained that in such a case $|R|^2 = |R_1|^2 + |R_2|^2 = 1$, $\bar{T} = 0$. The meaning of R^2 follows from the interpretation:

R^2 = Reflected acoustic energy flux (time averaged over 1 cycle)/Incident acoustic energy flux (time averaged over 1 cycle)

and is discussed in Appendix A.

The quantities A, B, C, and D in Eq. (13) are explicitly given by:

$$A = (1/4\tau)[f_\eta(0)g_\eta(1) - f_\eta(1)g_\eta(0)]$$

$$B = 4\tau\sqrt{\eta_0^2 - 1}\sqrt{\eta_1^2 - 1}\,[f(1)g(0) - f(0)g(1)]$$

$$C = \sqrt{\eta_1^2 - 1}[f(1)g_\eta(0) - f_\eta(0)g(1)]$$

$$D = \sqrt{\eta_0^2 - 1}[f_\eta(1)g(0) - f(0)g_\eta(1)] \tag{14}$$

For simplicity we have assumed $\sin\theta \geq 0$ in the expressions for A, B, C, and D given by Eqs. (14), since for the geometry chosen in Fig. 1 resonances and/or Brewster angles for the corresponding vortex sheet cases exist only for $0 \leq \theta \leq \pi/2$. Equations (14) may be made general, i.e., to apply for all values of the incidence angle $\theta(-\pi/2 \leq \theta \leq +\pi/2)$ by multiplying B and C by $\mathrm{sgn}(\sin\theta)$.

The upper signs in Eqs. (14) hold for $\eta_1 \geq 1$ and the lower signs for $\eta_1 \leq -1$, in both cases $|\eta_1| \geq 1$, and we have used the notation 0 and 1 in the arguments of f and g and their derivatives with the understanding that 0 designates evaluation at $\eta = \eta_0 = \eta|_{z=0} = 1/\sin\theta$ and 1 designates evaluation at $\eta = \eta_1 = \eta|_{z=z_1} = 1/\sin\theta - M_1$, i.e., at the two edges of the shear layer. Equations (13-14) are valid for $-\pi/2 \leq \theta \leq +\pi/2$ with the upper signs holding for the regime of ordinary reflection ($\eta_1 > 1$ and $R^2 < 1$) and the lower signs for the regime of the so-called amplified reflection ($\eta_1 \leq -1$, $R^2 \geq 1$). (For the total reflection regime $|R|^2 = 1$, $-1 \leq \eta_1 \leq +1$, $-\pi/2 \leq \theta \leq +\pi/2$.) It is seen from Eqs. (13) and (14) that we recover the three reflection regimes:

Ordinary reflection regime:

$$\eta_1 \geq 1,\quad R^2 \leq 1$$

Total reflection regime:

$$-1 \le \eta_1 \le -1, \quad R^2 = 1$$

Amplified reflection regime:

$$\eta_1 \le -1, \quad R^2 \ge 1$$

which agree with the results of Graham and Graham.[3] Indeed these regimes are the same as those found by Miles[8] and Ribner[9] for the limiting case of the vortex sheet ($\tau = 0$).

III. Numerical Evaluation of Energy Reflection Coefficient R^2

We have evaluated numerically the Whittaker M functions involved in the two independent solutions $f(\eta;\tau)$ and $g(\eta;\tau)$ of the pressure perturbation equation given by Eqs. (9) using the known series representations of f and g as given by Koutsoyannis[5] for relatively small values of η and τ whereas for large values of η and/or τ we have used a numerical technique outlined in Appendix B. Using these values we have then evaluated the functions A, B, C, and D given in Eqs. (14) and then the expression for the energy reflection coefficient R^2 given by Eqs. (13). In particular we have chosen ranges of the relevant problem parameters, i.e., angle of incidence θ, upper fluid Mach number M_1, and Strouhal number τ, for which the corresponding vortex sheet (for the same θ and M_1) has one or two resonances and/or one or no Brewster angle.

Figure 2 shows the behavior of the energy reflection coefficient R^2 for the limiting cases of the vortex sheet ($\tau = 0$) and geometrical acoustics ($\tau \to \infty$) for a typical incidence angle $\theta = 30$ deg, as a function of the variable $\eta_1 = (1/\sin\theta) - M_1 = 2 - M_1$ or as a function of the upper fluid Mach number M_1. As is known[8,9] the vortex sheet in this case has resonances at $\eta_1 = -1/\sin\theta$ and $\eta_1 = -1/\cos\theta$, i.e., for M_1 equal to 4 and 3.155, respectively, and a Brewster angle at $\eta_1 = +1/\cos\theta$, i.e., at $M_1 = 0.845$. In the geometrical acoustics limit ($\tau \to \infty$) the energy reflection coefficient R^2, as a function of η_1, degenerates into the Heaviside-type step function $R^2 = 1 - H(1-\eta_1)$, i.e., $R^2 = 1$ for $\eta_1 < 1$ and $R^2 = 0$ for $\eta_1 > 1$.

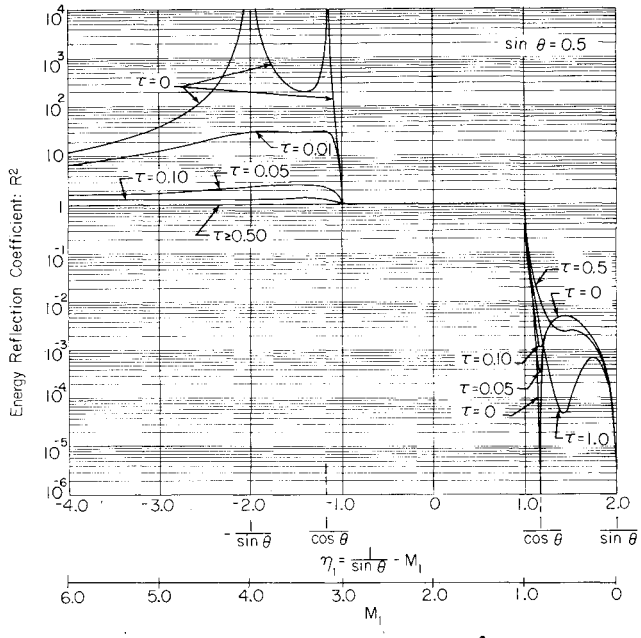

Fig. 3 Variation of energy reflection coefficient R^2 with upper fluid Mach number M_1 for incidence angle of $\theta = 30$ deg for various values of τ in interval $0 \le \tau \le 1$.

Figure 3 shows the variation of the reflection coefficient with upper fluid Mach number M_1 for a number of values of the parameter τ for a fixed angle of incidence of 30 deg. For 30 deg angle of incidence the corresponding vortex sheet ($\tau = 0$), as seen from Fig. 2, has two resonances, at $-1/\sin 30$ deg and $-1/\cos 30$ deg and one Brewster angle at $+1/\cos 30$ deg. It is seen from the figure that even for very small τ (~ 0.01) the resonances in the amplified reflection regime disappear and for values of $\tau \ge 0.5$ the amplified reflection regime has degenerated into the total reflection regime with $R^2 = 1$. In the ordinary reflection regime in which the

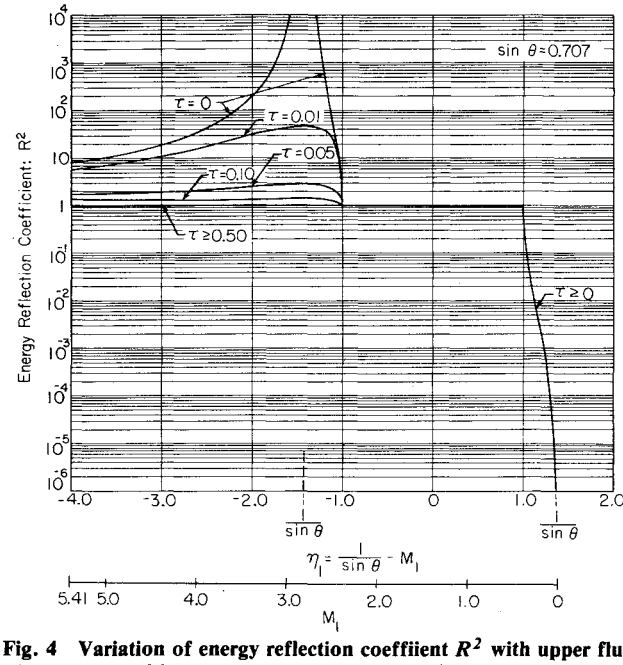

Fig. 4 Variation of energy reflection coeffiient R^2 with upper fluid Mach number M_1 for an angle of incidence $\theta = 45$ deg for various values of τ in range $0 \le \tau \le 1$. (Corresponding vortex sheet resonances and Brewster angles coalesce at $\eta_1 = -(1/\sin\theta)$ and $+(1/\sin\theta)$, respectively.)

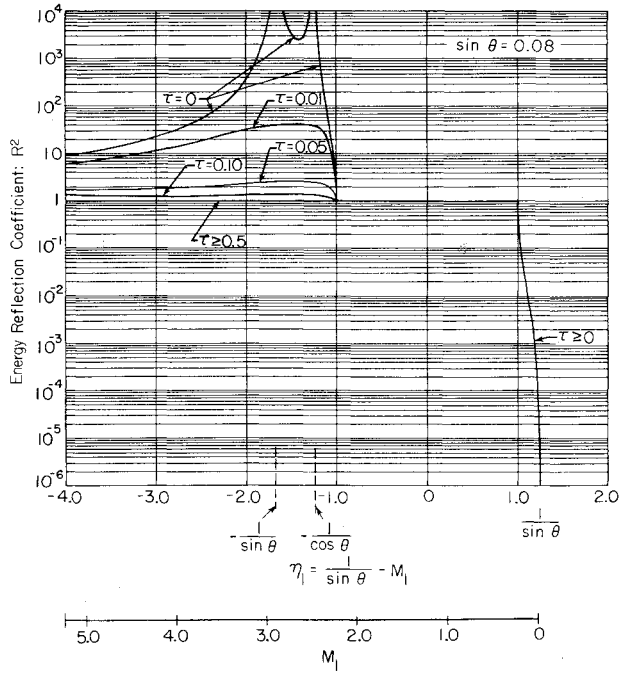

Fig. 5 Variation of energy reflection coefficient R^2 with upper fluid Mach number M_1 for incidence angle $\theta = \sin^{-1}(0.8)$ for various values of τ in interval $0 \le \tau \le 1$. (Corresponding vortex sheet has two resonances and one Brewster angle.)

corresponding vortex sheet has a Brewster angle at $\eta_1 = +1/\cos$ (30 deg), it is seen that even for low values of $\tau \sim 0.05$ the Brewster angle has disappeared and there is discernible variation of the reflection coefficient with upper fluid Mach number up to the value $\tau = 1$ that we have calculated.

Figure 4 shows the variation of the reflection coefficient with upper fluid Mach number M_1 for a number of values of the parameter τ and for a fixed angle of incidence of 45 deg. This is the special case in which the two resonances of the corresponding vortex sheet coalesce and the same holds for the Brewster angles. As in the 30 deg angle of incidence case we observe the same behavior in the amplified reflection regime, i.e., fast drop-off from the vortex sheet values with increasing τ and by $\tau \gtrsim 0.5$ the whole amplified reflection regime has coalesced with the total reflection one. In the ordinary reflection regime, however, we find essentially no variation from the vortex sheet values up to the value $\tau = 1$ calculated. Apparently it takes quite substantial values of $\tau > 1$ for the reflection coefficient to start differing from the values of the corresponding vortex sheet. Finally, Fig. 5 shows the variation of the reflection coefficient with upper fluid Mach number M_1 with τ as the varying parameter and for a fixed incidence angle θ for which $\sin\theta = 0.8$. The corresponding vortex sheet has two resonances and no Brewster angle. The general behavior is similar to that observed in Fig. 4, i.e., rapid decrease of reflection coefficient values with increasing τ in the amplified reflection regime and imperceptible change from the vortex sheet values in the ordinary reflection regime up to the value $\tau = 1$ calculated.

From the above figures the following general conclusions may be drawn. The finite-thickness shear layer shows no resonances and no Brewster angles. Moreover, the values of the reflection coefficient in the amplified reflection regime drop off substantially from those of the corresponding vortex sheet with increasing τ, even for modest values of τ on the order of ~ 1, whereas in the ordinary reflection regimes up to $\tau \sim 1$ modest or no significant changes are observed in the reflection coefficient values for the cases in which the corresponding vortex sheet exhibits no Brewster angle. In contrast when the corresponding vortex sheet exhibits a Brewster angle in the ordinary reflection regime, the reflection (and transmission) characteristics of the finite-thickness shear layer, as may be surmised from Fig. 3, strongly depend upon the value of the parameter τ (in addition to the angle of incidence θ and the upper fluid Mach number M_1). This is in contrast to the results of Graham and Graham[3] who, for the case of $M_1 = 3$ and $\sin\theta = 0.2$ which they examined as typical for the ordinary reflection regime, calculated negligible effects due to the finite thickness layer as compared with the corresponding vortex sheet results. The reason is, as may be easily checked, that in their case the corresponding vortex sheet had a Brewster angle at $\eta = 1/\cos\theta = 1.0206$, i.e., very close to 1 (see Fig. 2) and moreover they evaluated the variation of R and T as a function of the nondimensional parameter§

$$\frac{\text{Shear layer thickness}}{\text{Wave length}} = \frac{(\omega/a) z_1 \cos}{2\pi} = \frac{\omega}{b} \cdot \frac{bz_1}{a} \cdot \frac{\cos\theta}{2\pi}$$

$$= \frac{\omega}{b} M_1 \frac{\cos\theta}{2\pi}$$

§In actuality the parameter in Ref. 3 is:

$$\frac{\text{Shear layer thickness}}{(\text{Incident wave vector component in the } z \text{ direction})^{-1}}$$

$$= z_1 \Big/ \left[\left(\frac{1}{2\pi} \frac{\omega}{a} \cos\theta \right)^{-1} \right]$$

by considering variations of this parameter from zero to less than 0.2. This range corresponds to variations of our nondimensional parameter τ from zero to less than 0.02. Since the value $\tau = 0$ characterizes the vortex sheet, it follows that the choice of the this parameter in Ref. 3 was an unfortunate one,¶ and that the range of values of this parameter was too close to the vortex sheet value $\tau = 0$.

IV. Limiting Behavior of Reflection Coefficient

In this section we study analytically the limiting values and forms of the energy reflection coefficient R^2, as given by Eqs. (13), as a parameters τ, θ, and M_1 take extreme values by examining the behavior of A, B, C, and D in Eqs. (14) for these limiting values. In particular we are interested in $\tau \to 0$ or $\tau \to \infty$ corresponding to the vortex sheet and geometrical acoustics limits, respectively[5] (i.e., in $\theta \to 0$ or $\theta \to \pm\pi/2$ corresponding to the normal and parallel incidence, respectively) and in $M_1 \to 0$ or $M_1 \to \infty$ (i.e., the low and high upper fluid Mach number limits, respectively).

The vortex sheet limit $\tau \to 0$ follows from the known properties of the series solutions $f(\eta)$ and $g(\eta)$ in Eqs. (9) and from Eqs. (14).[5] In this limit $A \to 0$ and $B \to 0$, whereas

$$C \to 3\eta_0^2 \frac{\kappa \operatorname{sgn}\kappa}{\sqrt{1-\kappa^2}} \sqrt{\eta_1^2 - 1}$$

and

$$D \to -3\eta_1^2$$

and since $\kappa = \sin\theta$, $\eta_1 = (1/\sin\theta) - M_1$ we obtain from Eqs. (13)

$$R^2 = \left(\frac{C \pm D}{C \mp D} \right)^2$$

$$= \left[\frac{(1 - M_1\sin\theta)^2 \pm \sec\theta \sqrt{(1 - M_1\sin\theta)^2 - \sin^2\theta}}{(1 - M_1\sin\theta)^2 \mp \sec\theta \sqrt{(1 - M_1\sin\theta)^2 - \sin^2\theta}} \right]^2 \qquad (15)$$

where again M_1 is the upper fluid Mach number and upper signs correspond to ordinary reflection and lower signs to amplified reflection. Equation (15) is for the vortex sheet and agrees with the corresponding results obtained by Miles[8] and Ribner.[9]

The limiting form of the reflection coefficient in the limit of $\tau \to \infty$ (geometrical acoustics) may be obtained using the asymptotic form of the solutions $f(\eta)$ and $g(\eta)$ in Eqs. (9) as $\tau \to \infty$ (see Ref. 5). Instead of using these forms we may argue as follows: Since it has been shown that in the limit $\tau \to \infty$ one recovers both the amplitude and the phase function of geometrical acoustics,[5] it follows that the reflection coefficient R^2 in the limit $\tau \to \infty$ has the form consistent with geometrical acoustics, i.e.,

$$R^2 = 0 \text{ for } \eta_1 > 1$$

$$= 1 \text{ for } \eta_1 < 1 \qquad (16)$$

The limiting form for normal incidence (i.e., $\theta = 0$) is obtained by observing that in this limit

$$\eta_0 = \frac{1}{\sin\theta} \to +\infty, \quad \eta_1 = \frac{1}{\sin\theta} - M_1 \to +\infty$$

¶Since the parameter used in Ref. 3 does not contain the shear layer profile slope b, one could have anticipated that it was not a suitable nondimensional parameter to characterize adequately the scattering characteristics of the shear layer. In contrast our nondimensional parameter τ as given by Eq. (8) does characterize the essential features of the problem since it is the product of the Strouhal number ω/b and the sine of the angle of the incident wave vector with the z axis. (See also Ref. 5 for a detailed discussion of the physical meaning and importance of the parameter τ).

and also in Eqs. (14)

$$A \to 0, \quad B \to 0, \quad \text{and} \quad C \to -D$$

Consequently since only ordinary reflection is possible ($\eta_1 > 1$), the reflection coefficient is zero.

The limiting form for parallel incidence $\theta = \pm \pi/2$ (i.e., $\sin^2\theta = 1$) is obtained from Eqs. (14) by observing that in this limit

$$A \to \infty \quad \text{and} \quad C \to \infty$$

and the reflection coefficient is

$$R^2 \to \frac{A^2 + C^2}{A^2 + C^2} \to 1$$

The limiting form for $M \to 0$ is obtained again from Eqs. (14) by observing that in this limit

$$A \to 0, \quad B \to 0 \quad \text{and} \quad C \to -D$$

Consequently again only ordinary reflection is possible ($\eta_1 \to \eta_0 = 1/\sin\theta > 1$) with the reflection coefficient being zero.

Finally the limiting form of the reflection coefficient for $M \to \infty$ is the same as that for the vortex sheet [Eq. (15)], i.e., $R^2 = 1$ since in this case $\eta_1 \to -\infty$ and only the amplified reflection regime applies.

We summarize the above limiting forms of the values of the reflection coefficient together with the corresponding regimes (ordinary, total, or amplified reflection) in Table 1.

V. Resonances for Finite Thickness Thin Shear Layer

In this section we present a proof for the nonexistence of resonances for a nonzero but thin shear layer. It was seen from Eqs. (13) for the reflection coefficient R^2 that resonances which may exist only in the amplifying reflection regime ($\eta_1 < -1$) imply that

$$A + B = 0 \quad \text{and} \quad C + D = 0 \tag{17}$$

We found in deriving Eq. (15) for the vortex sheet case ($\tau = 0$) that, to the lowest order in τ, $A \to 0$ and $B \to 0$; whereas C and D are nonzero and yield the vortex sheet result. We next evaluated A and B to the lowest order in τ as follows: insert in Eqs. (14) the values for the functions $f(\eta)$ and $g(\eta)$ from Eqs. (9) to the lowest order in τ and then evaluate $A + B$ at the zeros of $C + D$. This shows that the two Eqs. (17) are incompatible for small but finite τ, so the only possibility remaining is that of $\tau = 0$, i.e., the vortex sheet case.

For small τ one may obtain from Eqs. (9)[5]

$$f(\eta;\tau) = 1 - (4\tau)^2\left(\frac{\eta^2}{2} + \frac{\eta^4}{4}\right) + O(\tau^4)$$
$$g(\eta;\tau) = \eta^3 + (4\tau)^2\left(\frac{\eta^5}{10} - \frac{\eta^7}{28}\right) + O(\tau^4) \tag{18}$$

Table 1 Limiting values of energy reflection coefficient R^2

	τ		θ		M_1	
	0	∞	0	$\pm\pi/2$	0	∞
Reflection coefficient R^2	Vortex sheet limit [Eq. (14)]	Geometrical acoustics limit	0	1	0	1
Reflection regime[a]	O, T, A	O, T, A	O	T, A	O	A

[a] O, T, or A are ordinary, total, and amplified reflection, respectively.

Inserting these values into Eqs. (14) we obtain:

$$A = (4\tau)[3(\eta_0 - \eta_1)\eta_0\eta_1(1 - \eta_0\eta_1)]$$
$$B = (4\tau)\sqrt{\eta_0^2 - 1}\,\sqrt{\eta_1^2 - 1}\,(\eta_0^3 - \eta_1^3) \tag{19}$$

Observing that $\eta_0 - \eta_1$ is the upper fluid Mach number M_1 we see from Eqs. (19) that the condition $A + B = 0$ yields:

$$A + B = (4\tau)[3\eta_0\eta_1(1 - \eta_0\eta_1) + \sqrt{\eta_0^2 - 1}\,\sqrt{\eta_1^2 - 1}\,(\eta_0^2 + \eta_1^2 + \eta_0\eta_1)] = 0 \tag{20}$$

Equation (20) must be evaluated at the vortex sheet values of η_0, i.e., where $C + D = 0$ at the vortex sheet values of η_0 and η_1. Using the two known properties of the vortex sheet solution,[8] i.e.,

$$\eta_0^2 + \eta_1^2 = \eta_0^2\eta_1^2, \quad \eta_0\eta_1 = 1 - \sqrt{M_1^2 + 1}$$

Equation (20) yields:

$$A + B = -(4\tau)(2M_1^3) = 0 \tag{21}$$

We see that Eq. (21) is satisfied only if $\tau = 0$ or $M_1 = 0$ or both and consequently the two Eqs. (17) required for the existence of resonances are incompatible to the lowest order in τ; it follows that the nonzero thickness thin shear layer has no resonances and no Brewster angles. The conditions for the existence of Brewster angles [i.e., $R^2 = 0$] is the same as that for the existence for resonances [i.e., Eqs. (17)], except that in this case the ordinary reflection regime ($\eta_1 > 1$) is the relevant on and the proof follows as for the case of the resonances.

One may also prove, in general, on the basis of certain differential properties of the quantities A, B, C, and D [Eqs. (14)] and the Wronskian properties of the solutions $f(\eta;\tau)$ and $g(\eta;\tau)$ [Eq. (9)] of Eq. (8), that not only the thin shear layer but also the finite-thickness shear layer has no resonances or Brewster angles and moreover resonances and Brewster angles are possible if and only if either $\tau = 0$ (the vortex sheet case) or $\tau \to \infty$ (the geometrical acoustics limit). See Fig. 2.**

VI. Conclusions

We have evaluated numerically the energy reflection coefficient for plane waves incident on a plane shear layer having a linear velocity profile. The numerical computations were based upon a representation of the pressure perturbations in the shear layer region in terms of Whittaker M functions.

We have found that the shear layer exhibits no resonances and no Brewster angles and that a separate analytical proof for the nonzero thickness but thin shear layer substantiates the absence of both resonances and Brewster angles for a finite-thickness layer. Moreover we have observed that the behavior of the reflection coefficient depends crucially upon the parameter τ, which, as is seen from Eq. (8), represents a nondimensional measure of the disturbance Strouhal number with respect to the disturbance Mach number in the mean flow direction. In particular for moderate values of τ, the amplified reflection regime degenerates into the total reflection one, whereas in the ordinary reflection regime the variation of the reflection coefficient with τ depends upon whether or not

**This is true not only for the linear shear layer [Eq. (1)] but also for a finite-thickness shear layer of a generally piecewise continuous velocity profile. This result and the corresponding studies will be published in a separate publication concerned with the scattering characteristics of finite-thickness shear layers with a piecewise continuous velocity profile, a special case of which is the shear layer with a linear mean velocity profile of the present study.

the corresponding vortex sheet has a Brewster angle. In cases in which the corresponding vortex sheet has a Brewster angle, the reflection coefficient is sensitive to changes in τ even for moderate values of τ, whereas in the cases in which the corresponding vortex sheet has no Brewster angle the reflection coefficient for moderate values of τ follows rather closely the corresponding vortex sheet values.

The above results indicate that caution should be exercised in modeling planar shear layers by vortex sheets uncritically even in the ordinary reflection regime and even for subsonic relative flows of the two regions bounding the shear layer, a practice customarily followed in current research and applications in noise studies and in aeroacoustics in general.[10] Although it is well known that the directional characteristics of the reflected and transmitted plane waves scattered by a finite-thickness plane parallel shear layer are independent of the details of the velocity profile in the layer (provided that the profile is "smooth") (see, e.g., Ref. 11), the amplitudes of the transmitted and reflected waves depend crucially upon the parameter τ, in addition to the angle of incidence θ and the relative Mach number M of the two uniform flows bounding the finite-thickness shear layer. Indeed we have shown that for certain combinations of τ, θ, and M, i.e., those for which the corresponding vortex sheet has a Brewster angle (energy reflection coefficient = 0), the scattering characteristics of a finite-thickness shear layer may differ drastically from those of the corresponding vortex sheet ($\tau = 0$) even for modest (nonzero) values of τ. Moreover if one allows for different densities and temperatures in the three flow regions ($z \le 0$, $0 \le z \le z_1$, and $z \ge z_1$), a case of particular interest to noise generation by and/or propagation through hot jets, the difference between the scattering characteristics of a finite-thickness shear layer and the corresponding vortex sheet characteristics becomes even more pronounced for certain ranges of values and/or combinations of the relevant parameters involved. The detailed calculations and the corresponding studies will be published in a separate publication concerned with the scattering characteristics of a linear shear layer as examined in the present studies but allowing for different densities ρ and speeds of sound a in the three regions of mean flow (see Fig. 1).

Finally, a connection could be made and an analogy drawn with internal gravity waves in a stratified fluid which exhibit "over-reflection" (what we have called, in this paper, amplified reflection), as exemplified in the work of Jones[12] Eltayeb and McKenzie,[13] and the more recent work of Acheson.[14] We believe though that such a connection will be confusing rather than illuminating. One of the reasons is that the basic notions underlying amplifying reflection in compressible and supersonic (as opposed to incompressible in the gravity wave analogy) parallel free shear layer flows are subtle but adequately understood for at least the compressible vortex sheet as exemplified by the work of Miles,[8] Howe,[15] and the extensive work of Jones.[16] For the finite-thickness shear layers the energetics and dynamics of amplified reflection are far from well understood and we plan to deal with this subject in another publication. (See the cautionary remarks in Acheson's[14] paper, at the footnote on p. 434††.)

Appendix A

Representation of Velocity Potentials in Regions $z \le 0$ and $z \ge z_1$

Velocity Potential ϕ_ℓ for Lower Region $z \le 0$

Consider that an incident plane wave with coordinates (x,z) fixed in the lower fluid, which is at rest, is a sine wave with a wave vector $\boldsymbol{k}$ making an angle θ with the z axis, i.e.,

$$\boldsymbol{k}\cdot\boldsymbol{e}_z = k\cos\theta \text{ with } -\frac{\pi}{2} \le \theta \le +\frac{\pi}{2}$$

The wave is an upcoming one with amplitude A and thus its potential may be written as:

$$\phi_i = \phi_{\text{incident}} = A\sin(k_x x + k_z z - \omega t)$$

and since $k_x = k\sin\theta$, $k_z = k\cos\theta$, and $k = \omega/a$ we may further write:

$$\phi_i = A\sin[(\omega/a)\,(x\sin\theta + z\cos\theta - at)]$$

The reflected wave will in general have in-phase and out-of-phase case components; thus since the x wave number is conserved in this stratified medium[8] we may write for the reflected wave which is a downward one:

$$\phi_r = \phi_{\text{reflected}} = A\{R_1\sin[(\omega/a)\,(x\sin\theta - z\cos\theta - at)] + R_2\cos(\omega/a)\,(x\sin\theta - z\cos\theta - at)\}$$

where R_1 and R_2 are, respectively, the in-phase and out-of-phase components of the reflection coefficient for the velocity potential. Finally

$$\begin{aligned}\phi_\ell &= \text{total velocity potential in the lower region } z \le 0\\ &= \phi_i + \phi_r\\ &= A\{\sin[(\omega/a)\,(x\sin\theta + z\cos\theta - at)]\\ &\quad + R_1\sin[(\omega/a)\,(x\sin\theta - z\cos\theta - at)]\\ &\quad + R_2\cos[(\omega/a)\,(x\sin\theta - z\cos\theta - at)]\}\end{aligned}$$

Defining by $\bar{R} = R_1 \pm iR_2$, the complex reflection coefficient, and taking the amplitude A to be real, we may write in complex notation[1]:

$$\begin{aligned}\phi_e &= A\text{R.P.}\{\pm i[e^{\pm i(k_x x + k_z z - \omega t)} + \bar{R}e^{\pm(k_x x - k_z z - \omega t)}]\}\\ &= A\text{R.P.}\{\pm i[\cos(k_x x + k_z z - \omega t) \pm i\sin(k_x x + k_z z - \omega t)]\\ &\quad + (R_1 \pm iR_2)[\cos(k_x x - k_z z - \omega t) \pm i\sin(k_x x - k_z z - \omega t)]\}\\ &= A\{\sin(k_x x + k_z z - \omega t) + R_1\sin(k_x x - k_z z - \omega t)\\ &\quad + R_2\sin(k_x x - k_z z - \omega t)\}\end{aligned}$$

irrespective of upper or lower signs.

Velocity Potential ϕ_u in Upper Region $z \ge z_1$

The upper medium is moving with uniform velocity $U_1 = bz_1\boldsymbol{e}_x$, with $M_1 = bz_1/a$, with respect to the (x,z) coordinate system fixed in the lower fluid (which is at rest).

Since again the x wave number is conserved in the stratified medium[8] we may write for the velocity potential of the transmitted wave:

$$\phi_u = A\{T_1\sin[k_{Tx}x + k_{Tz}(z - z_1) - \omega t] + T_2\cos[k_{Tx}x + k_{Tz}(z - z_1) - \omega t)]\}$$

where T_1 and T_2 are the in-phase and out-of-phase components of the transmitted wave. As before k_{Tx} is obtained from the x wave number conservation, i.e.:

$$k_{Tx} = k_T\sin\varphi = k_{ix} = k\sin\theta = (\omega/a)\sin\theta$$

††It is rather suprising that Acheson's 40-page paper, although based upon electromagnetic wave propagation concepts long employed in plasma physics, omits reference to the fundamental work of Briggs[17] who discussed very carefully criteria for amplifying waves and absolute instabilities as opposed to convective instabilities and their connection and who gave numerous examples as early as 1964.

where φ is the transmitted wave angle, but the z wave number k_{Tz} of the transmitted wave may only be uniquely specified by applying the radiation condition as postulated by Miles.[8] Namely from geometrical considerations,

$$k_{Tz}^2 = k_T^2 - k_{Tx}^2$$

i.e., $k_{Tz} = \pm\sqrt{k_T^2 - k_{Tx}^2}$, and k_T is then obtained from conservation of the frequency ω,[8] i.e., since φ is the angle that the transmitted wave vector makes with the z axis, then

$$\omega = ka = k_T c_T = k_T(a + U_1 \sin\varphi)$$

which together with the x wave number conservation, and phase speed conservation, i.e.,

$$\frac{a}{\sin\theta} = \frac{a}{\sin} + U_1$$

results in:

$$k_T = k(1 - M_1 \sin\theta)$$

Finally:

$$k_{Tz} = \pm\sqrt{k^2(1 - M_1\sin\theta)^2 - k^2\sin^2\theta} = \pm k\,|\sin\theta|\sqrt{\eta_1^2 - 1}$$

Which of the two signs in the expression for k_{Tz} is to be taken is determined by the radiation conditions as postulated by Miles,[8] i.e., $+$sign for $\eta_1 > 1$ in the so-called ordinary reflection regime and $-$sign for $\eta_1 < -1$ in the so-called amplifying reflection regime.

Finally writing $\bar{T} = T_1 \pm iT_2$ and substituting in the expression for ϕ_u we obtain the expression given by Eq. (3) in terms of the complex transmission coefficient $\bar{T}$.

Definition of Energy Reflection Coefficient

We define the energy reflection coefficient R^2 as

$$R^2 = \frac{\text{Ref. acoustic energy flux density ave. over cycle}}{\text{Inc. acoustic energy flux density ave. over cycle}}$$

And since for a plane wave propagating in a medium at rest the energy flux density is $a\rho_0 v'^2$, where v' is the (acoustic) particle velocity in the direction of the plane wave propagation, we may write:

$$v'^2_{\text{incident}} = \left(\frac{\partial\phi_i}{\partial x}\right)^2 + \left(\frac{\partial\phi_i}{\partial z}\right)^2$$

$$v'^2_{\text{reflected}} = \left(\frac{\partial\phi_r}{\partial x}\right)^2 + \left(\frac{\partial\phi_r}{\partial z}\right)^2$$

thus indicating with a bar time averaging over a cycle of the incident monochromatic wave:

$$R^2 = \overline{v'^2_{\text{reflected}}}\,/\,\overline{v'^2_{\text{incident}}}$$

$$= A^2\frac{\omega^2}{a^2}\left\{R_1^2\overline{\cos^2\left[\frac{\omega}{a}(x\sin\theta + z\cos\theta - at)\right]}\right.$$

$$\left. + R_2^2\overline{\sin^2\left[\frac{\omega}{a}(x\sin\theta - z\cos\theta - at)\right]}\right\}$$

$$+ \left\{A^2\frac{\omega^2}{a^2}\overline{\left[\cos^2\frac{\omega}{a}(x\sin + z\cos - at)\right]}\right\} = R_1^2 + R_2^2$$

Acoustic Energy Conservation

Much confusion has resulted in the literature concerning the precise expression and the meaning of acoustic energy conservation in a stratified fluid since the original publication of Blokhintzev's work.[18] The confusion has been compounded by Ribner's analysis[9] as well as by the more recent review by Candel.[19] It is actually a very simple matter to show that in parallel flows what is actually conserved is the time-averaged (over one cycle) cross-flow component of the energy flux density in a reference frame moving with the mean local speed, i.e., the conservation principle may be stated as follows:

$$\frac{\overline{pv'\cdot n_\perp}}{\omega'/\omega} = \text{const. (independent of } z)$$

where ω' accounts for the usual Doppler factor relating ω (in the $(x\text{-}z)$ frame) and ω' (in the moving frame), and $n_\perp$ is the unit normal to the parallel flow direction. The above relation relates to and compliments Bretherton and Garret's[20] action principle with the essential difference that whereas their principle is limited to short wavelengths, our result in the above equation (although limited to a statement concerning the time-averaged cross-flow part of the energy density flux of a single monochromatic component) is valid for all frequencies.

Since the proof of the above statement has not been given anywhere in the literature, we present below a sketch of this proof, with the details to be published elsewhere.

In a medium at rest

$$p' = -\rho_0\frac{\partial\phi}{\partial t} \quad \text{and} \quad v' = \nabla\phi$$

and

$$p'v\cdot e_z = -\rho_0\frac{\partial\phi}{\partial t}\frac{\partial\phi}{\partial z}$$

Thus for the lower region (which is at rest) we may write, since $\omega = \omega'$,

$$\left(\overline{\frac{p'v'\cdot e_z}{\omega'/\omega}}\right)_\ell = \frac{-\rho_0}{\omega}\overline{\frac{\partial\phi_\ell}{\partial t}\frac{\partial\phi_\ell}{\partial z}} = \frac{A^2\rho_0\omega}{2a}\cos\theta(1 - R^2)$$

Similarly for the upper region of uniform flow $U_1 = bz_1$, for which

$$p' = -\rho_0\frac{\mathrm{D}_1\phi_u}{\mathrm{D}t}, \quad v' = \nabla\phi_u$$

we obtain similarly:

$$\left(\overline{\frac{p'v'\cdot e_z}{\omega'/\omega}}\right)_u = \frac{-\rho_0}{\omega'}\overline{\frac{\mathrm{D}_1\phi_u}{\mathrm{D}t}\frac{\partial\phi_u}{\partial z}} = \frac{A^2\rho_0 k_{Tz}T^2}{2}\frac{\omega(1 - M_1\sin\theta)}{\omega'}$$

$$= \frac{A^2\rho_0 k_{Tz}T^2}{2}$$

Thus energy conservation follows,

$$(1 - R^2)k_{iz} = T^2 k_{Tz}$$

where $k_{iz} = k\cos\theta$, $k_{Tz} = \pm\sqrt{(1 - M_1\sin\theta)^2 - \sin^2\theta}$.

Appendix B: Numerical Evaluation of Solutions of $y'' + \left[1 - \frac{2\tau}{x} + \frac{1 - \mu^2}{4x^2}\right]y = 0$

We are concerned with the numerical evaluation of the solutions of the differential equation

$$y'' + \left[\frac{1}{4} - \frac{\tau}{x} + \frac{1 - \mu^2}{4x^2}\right]y = 0 \qquad \text{(B1)}$$

subject to the condition

$$\lim_{x\to 0} y(x)/x^{(1+\mu/2)} = 1 \tag{B2}$$

for arbitrary values of $x>0$, τ, and $\mu \neq -1, -2, -3, \ldots$

Although power and asymptotic series exist, they are not really useful for numerical work, especially for "large" values of τ and x. A much better approach is to use the three-term recurrence relation and normalization sum for numerical work. This approach allows a numerically stable, unitary, and computationally efficient algorithm which can be used over a very wide range of values of x and τ.

The solutions of Eq. (B1) and under the condition of Eq. (B2) are

$$S(\tau,+\mu;x) = M_{i\tau,\mu/2}(ix)/(i)^{(1+\mu/2)}$$

$$S(\tau,-\mu;x) = M_{i\tau,-\mu/2}(ix)/(i)^{(1-\mu/2)} \tag{B3}$$

where $M_{k,m}(z)$ is Whittaker's function.

Using Buchholz[21] we can show that the functions

$$u_j = S(\tau,\mu+2j;x)\,\frac{\Gamma(\mu+j)}{\Gamma(\mu+2j)}$$

satisfy the three-term recurrence relation

$$\left[\frac{\mu+j-1}{(\mu+2j-1)(\mu+2j-2)}\right]u_{j+1} - \frac{1}{x} + \left[\frac{2\tau}{(\mu+2j-1)(\mu+2j-2)}\right]u_j + \left[\frac{\tfrac{1}{4}(\mu+2j+1)^2+\tau^2}{(\mu+j)(\mu+2j+1)(\mu+2j+2)}\right]u_{j-1} = 0 \tag{B4}$$

and are subject to the normalization relation

$$\sum_{j=0}^{\infty} \lambda_j(\omega)\,u_j = e^{(\omega x/2)}\,x^{(1+\mu/2)} \tag{B5}$$

The $\lambda_j(\omega)$ are given by

$$\lambda_j(\omega) = (i)^j P_j^{(\mu-1)/2+i\tau,(\mu-1)/2-i\tau}(-i\omega) \tag{B6}$$

where $P_j^{(\alpha,\beta)}(x)$ are the Jacobi polynomials.

Equations (B4-B6) form the basis of the numerical algorithm. Using the Perron-Kresser theorem,[22] the solutions of Eq. (B4) behave asymptotically as

$$u_{j+1}/u_j \sim +\frac{4}{x}j \quad \text{or} \quad u_j/u_{j+1} \sim \frac{x}{4}j^{-1}$$

Using Eqs. (B5) and (B6), we infer that the required solution has the latter behavior; this solution is called the subdominant solution. The actual numerical algorithm is based upon the algorithm of Olver.[23,24]

Acknowledgment

The authors would like to express their appreciation to Ramji Digumarthi for his help in the computer plotting of Figs. 2-5. This work has been supported by the National Aeronautics and Space Administration under Grants 2007 and 676 to the Joint Institute for Aeronautics and Acoustics.

References

[1] Küchemann, D., "Störungsbewegungen in einer Gatrömung mit Grenzschicht," *Zeitschrift füre angewante Mathematik und Mechanik*, Vol. 18, 1938, pp. 207-222; see also Görtler, H., Vol. 23, 1943, p. 1.

[2] Pridmore-Brown, D. C., "Sound Propagation in a Fluid Flowing Through an Attenuating Duct," *Journal of Fluid Mechanics*, Vol. 4, 1958, pp. 393-406.

[3] Graham, E. W. and Graham, B. B., "Effect of a Shear Layer on Plane Waves of Sound in Fluid," *Journal of the Acoustical Society of America*, Vol. 46, No. 1, 1969, pp. 369-375.

[4] Goldstein, M. and Rice, E., "Effect of Shear on Duct Wall Impedance," *Journal of Sound and Vibration*, Vol. 30, No. 1, 1973, pp. 79-84.

[5] Koutsoyannis, S. P., "Characterization of Acoustic Disturbances in Linearly Sheared Flows," *Journal of Sound and Vibration*, Vol. 68 (2), Jan. 1980, pp. 187-202.

[6] Jones, D. S., "The Scattering of Sound by a Simple Shear Layer," *Philosophical Transactions*, Vol. 284A, 1977, pp. 287-328.

[7] Scott, J. N., "Propagation of Sound Waves Through a Linear Shear Layer," *AIAA Journal*, Vol. 17, 1979, pp. 237-244.

[8] Miles, J. W., "On the Reflection of Sound at an Interface of Relative Motion," *Journal of the Acoustical Society of America,* Vol. 29, 1957, pp. 226-228.

[9] Ribner, H. S., "Reflection, Transmission and Amplification of Sound by a Moving Medium," *Journal of the Acoustical Society of America*, Vol. 27, No. 4, 1957, pp. 435.

[10] Candel, S. M., "Application of Geometrical Techniques to Aeroacoustic Problems," AIAA Paper 76-546, Palo Alto, Calif., 1976.

[11] Kornhauser, E. T., "Ray Theory for Moving Fluids," *Journal of the Acoustical Society of America*, Vol. 25, No. 5, 1953, pp. 945-951.

[12] Jones, W. L., "Reflection and Stability of Waves in Stably Stratified Fluids with Shear Flow: A Numerical Study," *Journal of Fluid Mechanics*, Vol. 34, 1968, pp. 609-624.

[13] Eltayeb, I. A. and McKenzie, J. F., "Critical-Level Behavior and Wave Amplification of a Gravity Wave Incident Upon a Shear Layer," *Journal of Fluid Mechanics*, Vol. 72, 1975, pp. 661-671.

[14] Acheson, D. J., "On Overreflection," *Journal of Fluid Mechanics*, Vol. 77, 1976, pp. 433-472.

[15] Howe, M. S., "Transmission of an Acoustic Pulse Through a Plane Vortex Sheet," *Journal of Fluid Mechanics*, Vol. 43, 1970, pp. 353-367.

[16] Jones, D. S., "The Instability Due to Acoustic Radiation Striking on a Vortex Sheet on a Supersonic Stream," *Proceedings of the Royal Society of Edinburgh*, Series A, Vol. 71, No. 11, 1972-1973, pp. 121-140.

[17] Briggs, R. J., "Electron-Stream Interaction with Plasmas," Massachusets Institute of Technology Press, Cambridge, Mass., Research Monograph 29, 1964.

[18] Blokhintzeve, D. I., "Acoustics of a Nonhomogeneous Moving Medium," *Tekhniko-Theoreticheskoi Literatury, Moskva*, NACA TM 1399, 1946.

[19] Candel, S. M., "Acoustic Conservation Principles and an Application to Plane and Model Propagation in Nozzles and Diffusers," *Journal of Sound and Vibration*, Vol. 41, No. 2, 1975, pp. 207-232.

[20] Bretherton, F. P. and Garrett, C.J.R., "Wavetrains in Inhomogeneous Moving Media," *Proceedings of the Royal Society*, Vol. A320, 1969, pp. 529-554.

[21] Buchholz, H., *Die Konfluente Hypergeometrische Funktion*, Springer-Verlag, Berlin-Göttingen-Heidelberg, 1953.

[22] Schafke, F. W., "Lösengstypen von Difference Gleichungen und Summengleischungen in Normierten Abelchen Gruppen," *Mathematische Zeitschrift*, Vol. 88, 1965, pp. 61-104.

[23] Olver, F.W.J., "Numerical Solution of Second-Order Linear Difference Equation," *Journal of Research of the National Bureau of Standards*, Sec. B, Vol. 71, 1967, pp. 111-129.

[24] Olver, F.W.J. and Sookne, D., J., "Note on Background Recurrence Algorithms," *Journal of Mathematical Computations*, Vol. 26, 1972, pp. 941-947.